



Mathematical Modeling of Peristaltic Flow of Chyme in Small Intestine

Daniel N. Riahi and Ranadhir Roy

Department of Mathematics
University of Texas-Pan American
1201 W. University Dr.
Edinburg, TX 78539-2999
driahi@utpa.edu

Received: March 6, 2011; Accepted: July 25, 2011

Abstract

Mathematical models based on axisymmetric Newtonian incompressible fluid flow are studied for the peristaltic flow of chyme in the small intestines, which is an axisymmetric cylindrical tube. The flow is modeled more realistically modeled by assuming that the peristaltic rush wave is a non-periodic mode composed of two sinusoidal waves of different wavelengths, which propagate at the same speed along the outer boundary of the tube. Both cases of flow in a tube and in an annulus that are modeled and investigated in the present paper correspond respectively to the cases of flow of chyme in the small intestine in the absence and presence of a cylindrical endoscope. For the realistic values of the parameters for these two flow cases, we determine the expressions for the leading order pressure drop, the pressure, the axial velocity, and the frictional forces at the boundaries, and evaluated the roles played by these quantities in the investigated flow systems. The presence of the two-wave peristaltic mode was found to facilitate lower positive (adverse) pressure gradient and less magnitude of the forces by the boundaries on the flow of chyme.

Keywords: Math modeling, gastrointestinal, chyme flow, endoscopy, flow modeling, peristaltic flow

MSC 2010 No.: 92C10, 76Z

1. Introduction

Intestinal infection has become a rather common disease in living systems such as that of human. This illness is often caused by environmental pollution such as water pollution and can lead to constipation, distention, etc. Due to such infectious conditions, a strong wave called peristaltic rush develops which travels relatively long distances in a few minutes in the small intestine, which is a convoluted tube of about 6-7 m in length and average radius about 1.25 cm lying in the central and lower parts of the abdomen. The main functions of the small intestine in human, which is called the gastrointestinal tract, are digestion and absorption. It is known that endoscopy can be a powerful means in the diagnosis and management of various types of intestinal illnesses.

Although there have been a number of studies about the transport of chyme flow by the peristaltic rush wave (Latham, 1966; Shapiro & Jaffrin, 1969; Shukla et al., 1969; Jaffrin & Shapiro, 1971; Srivastava & Srivastava, 1984, 1985; Srivastava & Saxena, 1995; Srivastava, 2002), which the physiologists refer to as peristalsis, no theoretical and computational investigation of realistic cases for non-periodic peristaltic rush wave seem to have been carried out prior to the present study. Also relatively little is rigorously known about the adverse effect of an inserted endoscope on the chyme flow in the small intestine. Srivastava (2007) investigated a particular case of this problem for axisymmetric and Newtonian fluid flow and restricted it to the case of a periodic peristaltic rush wave in the form of one sine wave of long wavelength and calculated the pressure drop and the friction forces versus several parameters. In the present study, we consider, for the first time more extensions of the work by Srivastava (2007) to the cases of non-periodic peristaltic flow, which is likely to be the more realistic form of such a wave (Srivastava, 2007), either in the presence or in the absence of endoscope in the small intestine. We also calculate, in addition to the pressure drop and friction forces, the pressure and leading order flow velocity versus the independent variables and several parameters.

2. Formulation and Analysis

We consider the problems of axisymmetric incompressible Newtonian fluid flow in a tube, which could model that of the flow of chyme in the small intestine, and the flow in a cylindrical annulus, which could model that of the flow of chyme bounded at the outer boundary by the small intestine and at the inner boundary by an inserted cylindrical endoscope co-axial with the cylindrical intestine tube. We assume that a peristaltic rush wave mode composed of two sinusoidal waves with different periods but with the same speed travels down the wall of the outer tube, which corresponds to the boundary of the small intestine. Figure 1 presents the physical geometry for both flow in the tube in the limiting case where the inner radius $r_i=0$ and flow in the annulus where $r_i \neq 0$. We describe the geometry of the outer tube surface as

$$H(z, t) = r_o + A_1 \sin[(2\pi/\lambda)(z-ct)] + A_2 \sin[(2\pi/\eta)(z-ct)], \quad (1)$$

where r_o is the radius of the outer tube (intestine), A_1 and λ are the amplitude and the wavelength of the wave 1, respectively, A_2 and η are the amplitude and wavelength of the wave 2, respectively, c is the wave speed, t is the time variable and z is the axial variable.

Due to the geometry of the physical problem, we employ the cylindrical coordinate system. The governing equations for the continuity and the momentum of an axisymmetric Newtonian fluid flow in a fixed frame are given by White (1991)

$$\partial(ru)/\partial r + \partial(rw)/\partial z = 0, \quad (2a)$$

$$\sigma(\partial u/\partial t + u\partial u/\partial r + w\partial u/\partial z) = -\partial p/\partial r + \mu(\nabla^2 u - u/r^2), \quad \nabla^2 \equiv (1/r)\partial/\partial r(r\partial/\partial r) + \partial^2/\partial z^2, \quad (2b)$$

$$\sigma(\partial w/\partial t + u\partial w/\partial r + w\partial w/\partial z) = -\partial p/\partial z + \mu\nabla^2 w, \quad (2c)$$

where r is the radial variable, σ , the fluid density, μ the dynamic viscosity of the fluid, the radial velocity, w the axial velocity and p the pressure.

We now consider the governing system in the peristaltic mode frame of reference moving at speed c of both waves, so that (2a)-(2c) become

$$\partial(ru)/\partial r + \partial(rW)/\partial Z = 0, \quad (3a)$$

$$\sigma(\partial u/\partial t + u\partial u/\partial r + W\partial u/\partial Z) = -\partial p/\partial r + \mu(\nabla^2 u - u/r^2), \quad (3b)$$

$$\sigma(\partial W/\partial t + u\partial W/\partial r + W\partial W/\partial Z) = -\partial p/\partial Z + \mu\nabla^2 W, \quad (3c)$$

where

$$Z = z - ct, \quad W = w - c. \quad (3d)$$

The boundary conditions in the moving frame of reference are

$$u = 0, \quad W = -c \quad \text{at } r = r_i, \quad (4a)$$

$$u = \partial H/\partial t = W(r = H, Z, t)(\partial H/\partial Z), \quad W = -c \quad \text{at } r = H, \quad (4b)$$

where r_i is the radius of the inner cylinder (endoscope).

Next, we non-dimensionalize the governing equations (3a)-(3c) and the boundary conditions (4a)-(4b) using r_o , λ , $\lambda/(r_o c)$, c , λ/c , $(\lambda c \mu/r_o)$ as scales for radial distance, axial distance, radial velocity, axial velocity, time and pressure, respectively. The non-dimensional form of the governing equations and the boundary conditions are then given below for simplicity using the same symbols that were used before for the independent variables, flow velocity and pressure

$$\partial(ru)/\partial r + \partial(rW)/\partial Z = 0, \quad (5a)$$

$$\varepsilon^3 R_e (\partial u/\partial t + u\partial u/\partial r + W\partial u/\partial Z) = -\partial p/\partial r + \varepsilon^2 [(1/r)\partial/\partial r(r\partial u/\partial r) - u/r^2 + \varepsilon^2 \partial^2 u/\partial Z^2], \quad (5b)$$

$$\varepsilon R_e (\partial W / \partial t + u \partial W / \partial r + W \partial W / \partial Z) = -\partial p / \partial Z + [(1/r) \partial / \partial r (r \partial W / \partial r) + \varepsilon^2 \partial^2 W / \partial Z^2], \quad (5c)$$

$$u=0, W=-1 \text{ at } r=\delta, \quad (5d)$$

$$u= W(r=h, Z, t)(\partial h / \partial Z), W=-1 \text{ at } r=h \equiv 1 + \Phi_1 \sin(2\pi Z) + \Phi_2 \sin(2\pi \gamma Z), \quad (5e)$$

where $R_e = \sigma c r_o / \mu$ is the Reynolds number, $\varepsilon = r_o / \lambda$ is ratio of the length scale in the radial to that in the axial direction, $\delta = r_i / r_o$ is the annulus aspect ratio, $\Phi_1 = A_1 / r_o$ is the non-dimensional amplitude of the wave component 1, $\Phi_2 = A_2 / r_o$ is the non-dimensional amplitude of the wave component 2, and $\gamma = \lambda / \eta$ the wavelength ratio between the two waves, which referred to as waves 1 and 2 hereafter. We assume that γ is a small parameter ($\gamma < 1$), so that the wavelength of the wave 2 is larger than that of the wave 1.

We shall assume that the Reynolds number R_e is sufficiently small and ε is also a small parameter, so our leading order investigation neglects terms in (5b)-(5c) that contain these parameters. The assumptions are consistent with the available observation (Lew et al., 1971) that R_e is very small and long wavelength approximation also exists in the small intestine. Under such assumptions, the equation (5b) implies that the pressure p is independent of the radial variation to the leading terms, and the equation (5c) can be integrated twice with respect to r leading to the result

$$W = -1 - 0.25(dp/dZ)[\delta^2 - r^2 + (\delta^2 - h^2) \ln(r/\delta) / \ln(\delta/h)], \quad (6a)$$

once the necessary boundary conditions given in (5d)-(5e) are used. For flow in the tube case, where $\delta = 0$, the expression for W has the form

$$W = -1 + 0.25(dp/dZ)(r^2 - h^2). \quad (6b)$$

Since the radial component of the flow velocity is small of order ε , the magnitude of the axial velocity given by (6a-b) represents the leading order magnitude of the velocity vector in the flow system.

Next, the dimensionless volume flow rate $q = \int_S W dS$, which is assumed to be given, in the wave frame (moving frame) along the axial direction is determined. Here S is the cross-sectional area of the annulus. We then find

$$q = \pi (\delta^2 - h^2) \{1 + 0.125(dp/dZ)[\delta^2 + h^2 - (\delta^2 - h^2) / \ln(\delta/h)]\}. \quad (7)$$

Now, the relation between the q in the moving frame and q_L in the laboratory frame (fixed frame), which is the instantaneous one, is

$$q = q_L - 2\pi \int_{\delta}^h r dr = q_L - \pi(h^2 - \delta^2). \quad (8a)$$

The relation between the mean volume flow rates given by

$$Q = \int_0^1 q_L dZ \quad (8b)$$

in the laboratory frame and q can then be found by taking the average of (8a), which yields the following equation:

$$q = Q - \pi(\langle h^2 \rangle - \delta^2), \quad (8c)$$

where

$$\langle h^2 \rangle \equiv \int_0^1 (h^2) dZ. \quad (8d)$$

The result (8c) is the extension of periodic peristaltic single-wave case for the flow in the tube (Shapiro et al., 1969) to the present case of non-periodic peristaltic two-wave case for either flow in the tube or flow in the annulus.

Using (7), we can solve for dp/dZ and then integrate in Z to find the expression for the pressure in the form

$$p = \int_0^Z G(Z) dZ + p_0, \quad (9a)$$

$$G(Z) \equiv \{8[Q/\pi + h^2 - \langle h^2 \rangle] / [\delta^4 - h^4 - (\delta^2 - h^2)^2 / \ln(\delta/h)]\} \text{ for } \delta > 0, \quad (9b)$$

$$G(Z) \equiv -\{8[Q/\pi + h^2 - \langle h^2 \rangle] / h^4\} \text{ for } \delta = 0, \quad (9c)$$

where p_0 is a constant. The expression for the pressure drop $\Delta p \equiv p(0) - p(1)$ across one wavelength is then found from (9a) to be

$$\Delta p = -\int_0^1 G(Z) dZ. \quad (9d)$$

This is essentially the same expression as the one obtained in Srivastava (2007) for the single peristaltic sinusoidal wave case after a rescaling that was used in that work for q was taken into account. Using (9a) to find dp/dZ and applying the result in (6a-b), we find the following respective expressions for leading order flow velocity:

$$W = -1 - 0.25 G(Z) [\delta^2 - r^2 + (\delta^2 - h^2) \ln(r/\delta) / \ln(\delta/h)] \text{ for } \delta > 0, \quad (10a)$$

$$W = -1 + 0.25 G(Z) (r^2 - h^2) \text{ for } \delta = 0. \quad (10b)$$

Frictional forces F_i and F_o at the inner and outer boundaries, respectively, can be found from the integration of the shear stress around each tube and over one wavelength in the axial direction (Landau & Lifshitz, 1987). In analogy to the flow over a planar surface, we consider integral over one wavelength along the Z -direction of the dimensionless dominated term $\partial W / \partial y$ for the shear stress over the plate, where $y+r = r_o$. This lead to the expressions for these forces that are given below

$$F_i = -\int_0^1 \pi G(Z) \{ \delta^2 - (\delta^2 - h^2) / [2 \ln(\delta/h)] \} dZ \text{ for } \delta > 0, \quad (11a)$$

$$F_o = -\int_0^1 \pi G(Z) \{ h^2 - (\delta^2 - h^2) / [2 \ln(\delta/h)] \} dZ. \quad (11b)$$

It should be noted that the already known results for the simple case of periodic peristaltic single wave in the tube can be found by taking the limits $\Phi_2 \rightarrow 0$ and $\delta \rightarrow 0$ in (9c)-(9d) and (11a)-(11b). This leads to

$$\Delta p = \int_0^1 G_0(Z) dZ, \quad G_0(Z) \equiv \{ 8[Q/\pi + (h^2 - 1 - \Phi_1^2/2)]/h^4 \}, \quad F_i = 0, \quad F_o = \int_0^1 \pi h^2 G_0(Z) dZ, \quad (12a-d)$$

which are similar to the results due to Srivastava and Saxena (1995) for a single sinusoidal wave and for the flow in the tube case after the relation (8c) is used to write Q in terms of q .

3. Results and Discussion

The numerical results for the pressure drop, the frictional forces and the leading order flow velocity and pressure given by the expressions (9)-(11) are determined by first developing a computer code for the numerical integrations of these equations, which led to generated data for the pressure and the flow velocity as functions of r and z and pressure drop and the frictional forces for given values of the flow rate, amplitudes of wave 1 and wave 2, the aspect ratio of the wavelengths of the two waves and the aspect ratio of the annulus. Here a positive pressure drop ($\Delta p > 0$) means that pressure in the chyme flow decreases with increasing Z , while a negative pressure drop ($\Delta p < 0$) means that pressure in the chyme flow increases with Z . Due to the nature of the annulus flow and the way the expressions for F_i and F_o are determined in the previous section, it should be noted that a positive value of the inner friction force ($F_i > 0$) means this force is acted by the endoscope on the chyme flow, while $F_i < 0$ means there is such a force acted by the chyme flow on the endoscope. However, in the case of the outer friction force, a negative value of F_o ($F_o < 0$) means that such force is acted by the intestine on the chyme flow, while a positive value of such force means that the chyme flow applies such force on the intestine.

3.1. Results for Pressure Drop and Frictional Forces for $\Phi_2 = 0$

We briefly present the typical results that obtained under the restriction that only one peristaltic single wave exist, so that we set $\Phi_2 = 0$. Our collected first set of the computational data for the pressure drop, the inner friction force and the outer friction force versus the flow rate for different values of the amplitude of the single wave and for both cases of the flow in the tube and the flow in the annulus. We found that the pressure drop is generally positive, provided the flow rate is not sufficiently small. Otherwise, the pressure drop is negative. Comparing these results for the case of flow in the tube, where $\delta = 0$, and the case of such flow in the annulus, we found that the magnitude of the pressure drop is generally smaller in the tube case. The inner friction force was found to be generally negative, provided the flow rate is not sufficiently small. Otherwise, F_i is positive. In contrast, the results for the outer friction force was found to be generally positive, provided Q is not too small. Otherwise, F_o becomes negative. Comparing

these results for the case of the flow in the tube and the case of the flow in the annulus, we found that the magnitude of the outer friction force is generally smaller in the tube system.

Our second set of collected computational data were for the pressure drop, the inner friction force and the outer friction force versus the amplitude of the single wave and for different values of the flow rate in the cases of either flow in the tube or in the annulus. We found that for sufficiently small amplitude, the pressure drop is positive but is smaller for smaller aspect ratio and higher Q . However, for sufficiently larger amplitude, the pressure drop can be negative. The results for the inner friction force indicate that for sufficiently small amplitude, the inner friction force is negative, and the magnitude of this force is larger for smaller Q and larger aspect ratio. For sufficiently small amplitude of the wave, the outer friction force is positive with smaller magnitude corresponding to larger Q and smaller aspect ratio. The present results for the flow in the tube agree, in particular, with those determined by Srivastava & Saxena (1995) in the Newtonian fluid limit.

3.2. Results for Pressure Drop and Frictional Forces at $\gamma = 0.1$

In this and the following two sub-sections, we present the results for the main topic of the present study for the flow in the tube and the flow in the annulus, which is about presence of the peristaltic rush mode composed of two waves 1 and 2 with different wavelengths but moving at the same speed. Figures 2-4 presents some typical results for the pressure drop, the inner friction force in the case of flow in the annulus and the outer friction force versus the flow rate for $\Phi_1 = 0.2$ but for different values of the amplitude of the wave 2 and the aspect ratio. It can be seen from Figure 2 that for the flow in the tube case, the pressure drop is positive and increases with the flow rate. This means that naturally higher flow rate is driven by higher pressure force and the pressure force drives the chyme in the direction of the peristaltic mode. For the flow in the annulus case, the pressure drop increases with Q and is negative only for sufficiently small flow rate. Thus, in the presence of the endoscope, direction of the driving pressure force could be reversed if the flow rate is sufficiently small. Comparing these results to the corresponding ones for the single wave case, we found that for the flow in the tube case, the presence of two waves eliminates negative values for the pressure drop, and the magnitude of the pressure drop is smaller. For the case of flow in the annulus, the magnitude of the pressure drop is generally smaller in the case of peristaltic mode of two waves.

It can be seen from Figure 3 that for the flow in the annulus case, the inner friction force F_i is generally negative if the flow rate is not too small. Otherwise, F_i is positive. Also, the magnitude of this force increases mostly with decreasing the amplitude of the second wave. Since the average flow rate for humans is not too small (Shukla et al., 1980), these results indicate that the flow of chyme applies a force on the endoscope, and the magnitude of this force decreases with increasing strength of the second wave. The results shown in Figure 4 indicate that the outer friction force increases with the flow rate, and this force is positive if the flow rate is not too small. Thus, the flow of chyme applies a force on the intestine. For the flow in either the tube or the annulus, this force is smaller if the amplitude of the second wave is larger. The outer friction force has higher magnitude in the annulus flow case, provided the flow rate is not too small. Thus, in the presence of the endoscope, the chyme applies a larger force on the intestine.

Figures 5-7 present some typical results for the pressure drop, the inner friction force in the case of the annulus flow and the outer friction force versus the amplitude of the first wave and for different values of the flow rate and the aspect ratio parameter. It can be seen from Figure 5 that the pressure drop is positive for not too large value of Φ_1 , and it decreases with increasing the amplitude of the first wave. The rate of decrease of Δp is higher for the annulus flow case. Thus, the driving force by the negative pressure gradient on the chyme in the direction of the peristaltic mode decreases if the strength of the wave l increases. Our generated data for the pressure drop indicated that for sufficiently larger amplitude of the first wave, the pressure drop becomes negative. Comparing these results with the corresponding ones for the single wave case, we found, in particular, that presence of two waves increases the domain in the amplitude of the first wave where the pressure drop is positive. The results shown in Figure 6 for the inner friction force in the annulus flow case indicate that F_i increases with the amplitude Φ_1 , and its value is negative for not too large value of Φ_1 . In addition, F_i is smaller for larger value of δ , provided Φ_1 is not too large. Comparing these results with the ones for the single wave case, we found, in particular, that presence of two waves requires higher value of Φ_1 before the inner friction force becomes positive. The results shown in Figure 7 for the outer friction force indicate that F_o is positive for not too large values of the amplitude of the first wave, decreases with increasing Φ_1 and is larger for larger flow rate. The rate of decrease of this force with respect to Φ_1 is higher for the flow in the annulus case. Comparing these results with those for the single wave case, we found, in particular, that presence of two waves requires, in general, higher values of Φ_1 before the outer friction force becomes negative.

3.3. Results for Pressure Drop and Friction Forces at $\gamma=0.4$

Figures 8-13 present results analogous to those presented in Figures 2-7 but for $\gamma = 0.4$. Comparing the results shown in Figures 8-10 to the corresponding ones for Figures 2-4, we found that the lower wavelength of the second wave leads to larger domain for the flow rate for which the pressure drop remains negative, the inner friction force (in the case of flow in the annulus) remains positive and the outer friction force remains negative. Comparing the results shown in Figures 11-13 to the corresponding ones for Figures 5-7, we found that the lower wavelength of the second wave leads to smaller domain for Φ_1 for which the pressure drop remains positive, the inner friction force (in the case of the annulus flow) remains negative and the outer friction force remains positive.

3.4. Results for Leading Order Velocity and Pressure

We generated data for the leading order flow velocity and pressure versus axial variable and for both annulus and tube flows and for different values of the amplitudes of the two waves, the flow rate, the aspect ratio parameter and the wavelength parameter. Figures 14-15 present some typical results for the pressure versus the axial variable with domain over one wavelength of the first wave. Here, $\Phi_1 = \Phi_2 = 0.2$, $\delta = 0.0, 0.44$ and $Q = 0.6, 2.0$. Figure 14 presents results for $\gamma = 0.1$. It can be seen from this figure that for the flow in the tube case, the pressure is lower for higher flow rate, which physically is understandable, and p mostly decreases with increasing Z

especially at higher flow rate. For the annulus flow, again p is lower for higher flow rate and decreases with increasing Z for higher flow rate. These qualitative results appear to hold for $\gamma = 0.4$ case presented in Figure 15. However, for $Q = 2$ the rate of decrease of p with respect to Z is lower for higher γ case.

Figures 16 and 17 present some typical results for the leading order velocity w in the fixed frame versus r for r between δ and h and $Z = 0.5$ with the same parameter values as those given for Figures 14 and 15, respectively. It can be seen from Figure 16, which is drawn for $\gamma = 0.1$, that $w > 0$ and as expected the flow velocity is higher for higher flow rate. The axial velocity for the flow in the tube case is higher than that for w in the annulus only if r is sufficiently small. The results for the case of $\gamma = 0.4$ shown in Figure 17 indicate somewhat similar results to those shown in Figure 16, except that the value of w is slightly higher for higher γ value. Figures 18 and 19 present some typical results for w versus Z over one wavelength of the first wave and $r = 0.5$ with the same parameter values as those given for Figures 16 and 17, respectively. It can be seen from Figure 18, which is for the case of $\gamma = 0.1$, that again the value of the flow velocity is higher for higher Q . For the flow in the tube case, the flow direction is from left to the right, except in the case of low flow rate where the flow is to the left with relatively small magnitude in an intermediate zone in the axial direction. It is expected that in this zone flow circulates slightly. Similar results are apparent in the case of the flow in the annulus. However, the magnitude of the axial velocity is mostly higher in the tube. The results for the case of $\gamma = 0.4$ (Figure 19) indicate similar trend as those given in Figure 18, except that some slight lower values of the magnitude of w is seen in the case of higher value of γ .

4. Conclusion and Remarks

Models based on the axisymmetric Newtonian incompressible fluid flow for both cases of the flow was developed and analyzed in the tube with application of chyme motion in the small intestine and the flow in the annulus with application of flow of chyme between the small intestine and an inserted cylindrical endoscope. We modeled the peristaltic flow in the form of a more realistic non-periodic peristaltic rush mode composed of two sinusoidal waves of different wavelengths that both travel at the same speed along the boundary of the small intestine. Our generated data provided information about the pressure, pressure drop, leading order flow velocity and the associated frictional forces at the boundaries. For the case of humans where the average flow rate is not too small, we found, in particular, that the pressure drop is generally positive and increases with the flow rate, and the flow pressure decreases with increasing the axial variable indicating that the driving pressure gradient force is along the peristaltic waves. Presence of the non-periodic peristaltic mode appears to enhance the driving force. The magnitudes of the frictional forces appear to be reduced if the strength of the second wave is increased. If the wavelength of the second wave is too large in comparison to that of the first wave, then the results are more realistic and there is larger domain in the flow rate where the pressure drop is positive and the frictional forces are mostly those acting by the chyme on the boundary, and the presence of non-periodic peristaltic mode appears to enhance such results.

As was partly referred to in the sections 1-3, in the case of a single peristaltic sinusoidal wave and in the Newtonian fluid limit, there have been calculations of pressure drop and friction force in the past (Shapiro et al., 1969; Shukla et al., 1980; Srivastava and Saxena, 1995; Srivastava,

2007). However, it is known for over four decades (Lew et al., 1971; Vander et al., 1975; Srivastava and Srivastava, 1985) that the peristaltic waves along the wall of the small intestine are more general than just a very simple periodic sinusoidal wave. Thus, our present results in the presence of a non-periodic rush mode are expected to be closer to the more realistic cases.

Finally it should be noted that the present study for the peristaltic flow of chyme was restricted to the Newtonian fluid flow and the axisymmetric cases. However, since the actual boundary of the small intestine is not purely axisymmetric, a more realistic consideration for such flow system will be to consider non-axisymmetric flow system of either Newtonian fluid or a more realistic power-law fluid (Srivastava and Srivastava, 1985; White, 1991). In addition, the case of moving boundary conditions can provide further applicability of the results to other biomedical, biological and engineering applications. It is hoped that such interesting extensions, which are possible to be carried out using a method of approach similar to the present one, will subsequently be pursued by authors in the future.

REFERENCES

- Jaffrin, M. Y. & Shapiro, A. H. (1971). Peristaltic pumping, *Ann. Rev. Fluid Mech.*, **3**, pp. 13-36
- Landau, L. D. & Lifshitz, E. M. (1987). *Fluid Mechanics*, Second Edition, Pergamon, London, UK
- Latham, T. W. (1966). Fluid motion in a peristaltic pump, M.S. Thesis, M.I.T., Cambridge, MA
- Lew, H. S., Fung, Y. C. & Lowenstein, C. B.(1971). Peristaltic carrying and mixing of chyme in small intestine, *J. Biomechanics*, **4**, pp. 297-315
- Shapiro, A. H., Jaffrin, M. Y. & Weinberg, S. L.(1969). Peristaltic pumping with long wavelength and low Reynolds number, *J. Fluid Mech.*, **37**, pp. 799-825
- Shukla, J. B., Parihar, R. S. & Rao, B. R. P.(1980). Effects of peripheral-layer viscosity on peristaltic transport of a bio-fluid, *J. Fluid Mech.*, **97**(2), pp. 225-237
- Srivastava, V. P. (2002). Particle-fluid suspension flow induced by peristaltic waves in a circular cylindrical tube, *Bull. Cal. Math. Soc.*, **5**, pp.167-184
- Srivastava, V. P. (2007). Effects of an inserted endoscope on chyme movement in small intestine-A theoretical model, *Applications and Applied Math.: An Int. J.*, **2**(2), pp. 79-91.
- Srivastava, V. P. & Saxena, M.(1995). A two-fluid model of non-Newtonian blood flow induced by peristaltic waves, *Rheologica Acta*, **34**, pp. 406-414
- Srivastava, L. M. & Srivastava, V. P.(1984). Peristaltic transport of blood Casson model II, *J. Biomechanics*, **17**, pp. 821-829
- Srivastava, L. M. & Srivastava, V. P.(1985). Peristaltic transport of a non-Newtonian fluid: applications to vas deferens and small intestine, *Annals Biomed. Eng.*, **13**, pp. 137-153.
- Vander, A. J., Sherman, J. H. & Luciano, D. (1975). *Human Physiology: The Mechanism of Body Function*, Tata McGraw-Hill Publication Company, New Delhi.
- White, F. M. (1991). *Viscous Fluid Flow*, McGraw-Hill Publication Inc., New York

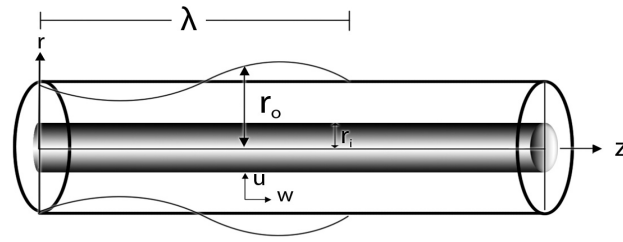


Figure 1. This is a schematic diagram for the physical system.

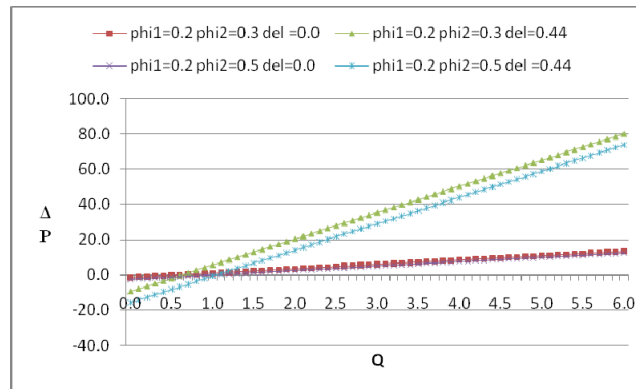


Figure 2. Pressure drop Δp versus the flow rate Q with the aspect ratio $\delta = 0, 0.44$ and the wave amplitude $\Phi_2 = 0.3, 0.5$. Here $\Phi_1 = 0.2$, $\gamma = 0.1$, and the symbols phi1, phi2 and del in the figure represent, respectively, Φ_1 , Φ_2 and δ .

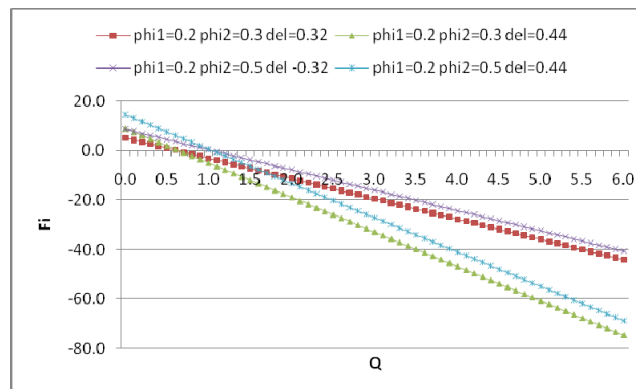


Figure 3. The same as in Figure 2 but for inner friction force F_i with $\delta = 0.32, 0.44$.

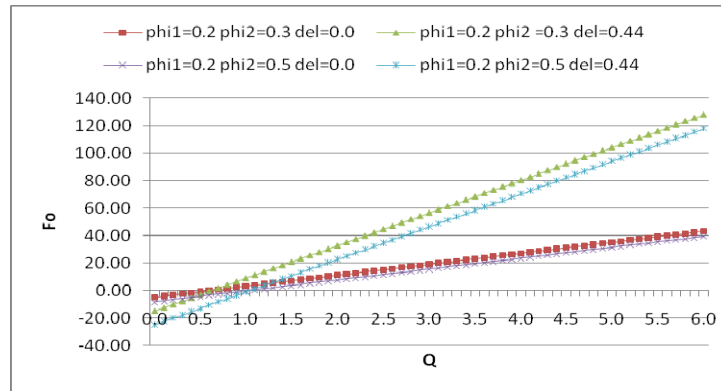


Figure 4. The same as in Figure 2, but for the outer friction force F_o .

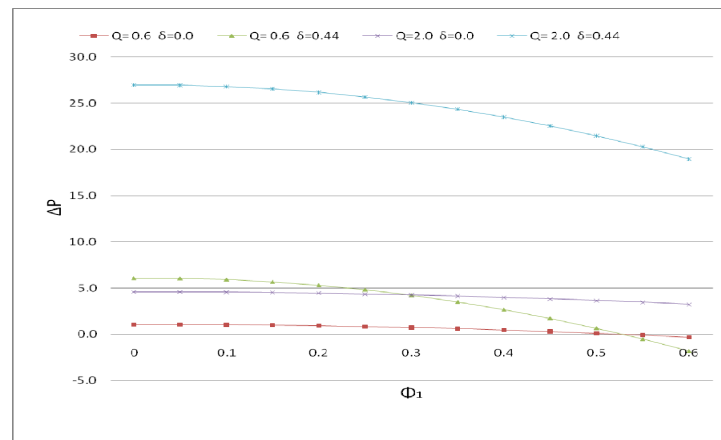


Figure 5. The pressure drop versus Φ_1 for $Q=0.6, 2.0, \Phi_2=0.1, \gamma=0.1$ and $\delta=0, 0.44$.

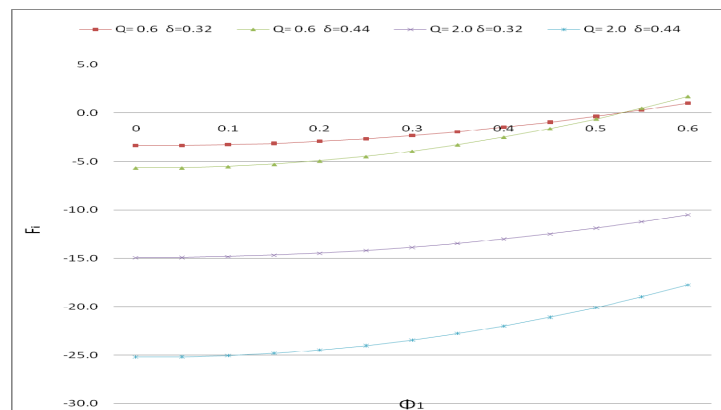


Figure 6. The same as in Figure 5, but for the inner friction force and $\delta=0.32, 0.44$.

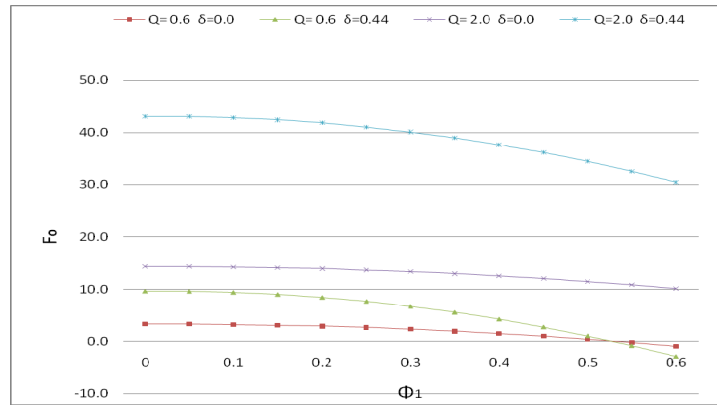


Figure 7. The same as in Figure 6, but for the outer friction force.

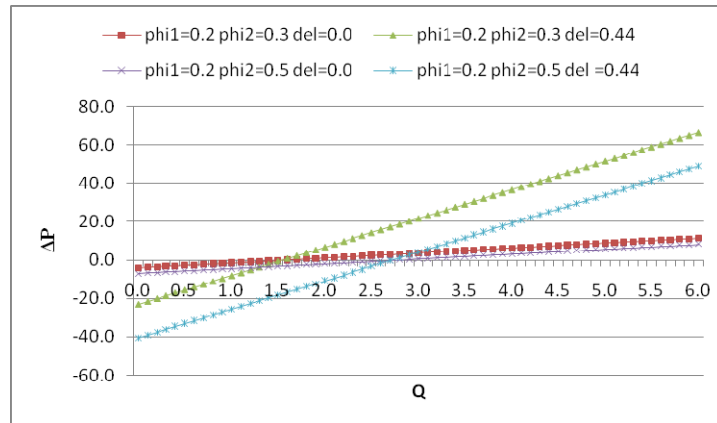


Figure 8. The same as in Figure 2, but for $\gamma = 0.4$.

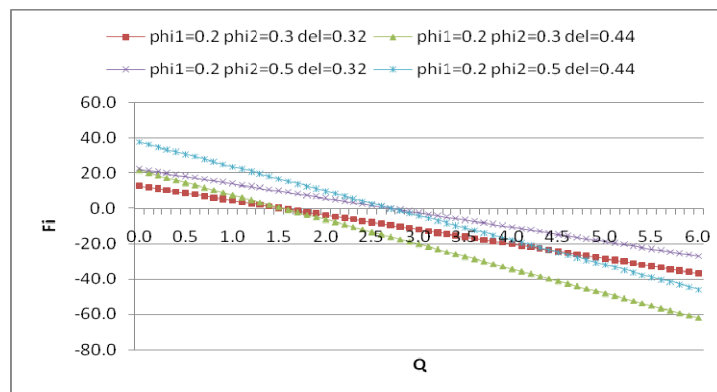


Figure 9. The same as in Figure 3, but for $\gamma = 0.4$.

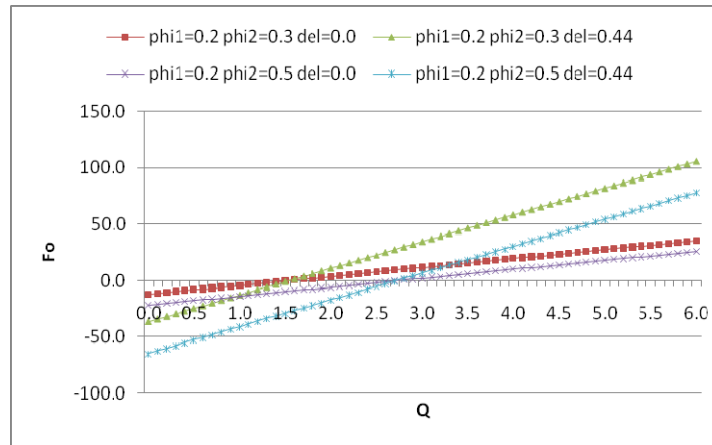


Figure 10. The same as in Figure 4, but for $\gamma = 0.4$

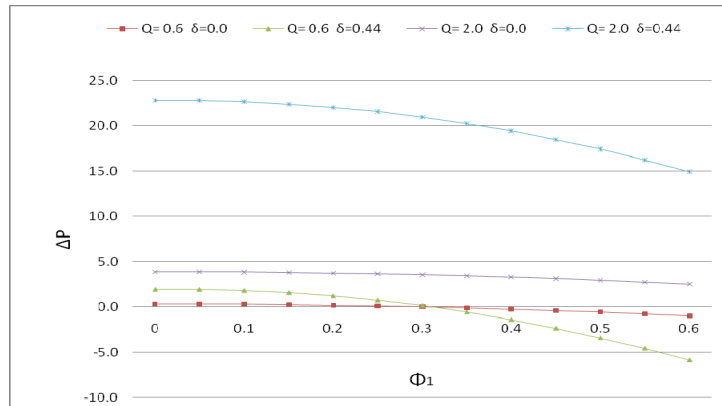


Figure 11. The same as in Figure 5, but for $\gamma = 0.4$.

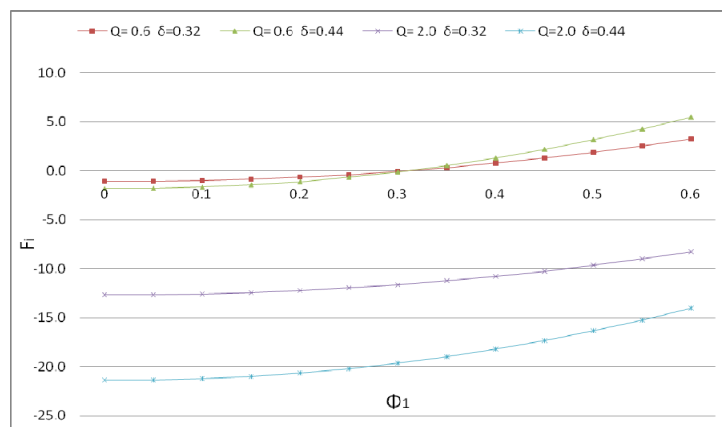


Figure 12. The same as in Figure 6, but for $\gamma = 0.4$.

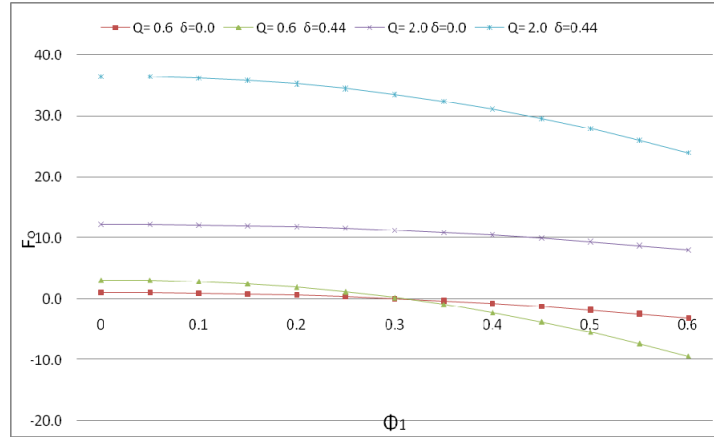


Figure 13. The same as in Figure 7, but for $\gamma = 0.4$.

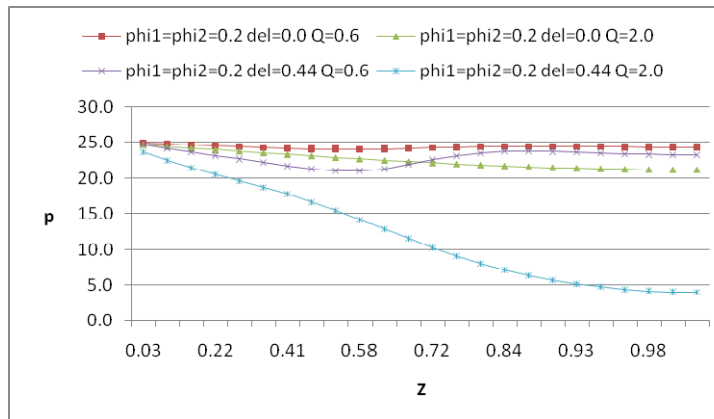


Figure 14. Pressure versus axial variable Z for $\Phi_1=\Phi_2=0.1$, $\gamma=0.1$, $\delta=0, 0.44$ and $Q=0.6, 2$. The symbols ϕ_1 , ϕ_2 and δ given in the figure refer to Φ_1 , Φ_2 and δ , respectively.

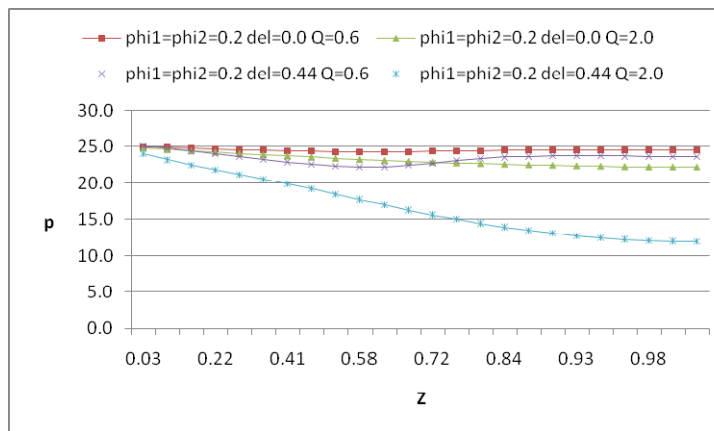


Figure 15. The same as in Figure 14, but for $\gamma = 0.4$.

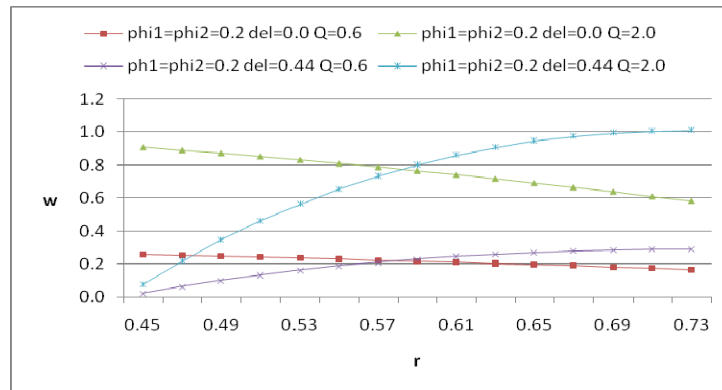


Figure 16. The same as in Figure 14, but for axial velocity w versus r at $Z=0.5$.

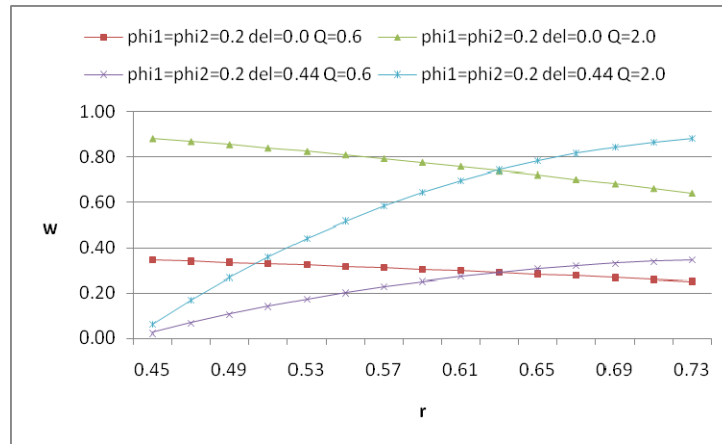


Figure 17. The same as in Figure 15, but for w versus r at $Z=0.5$.

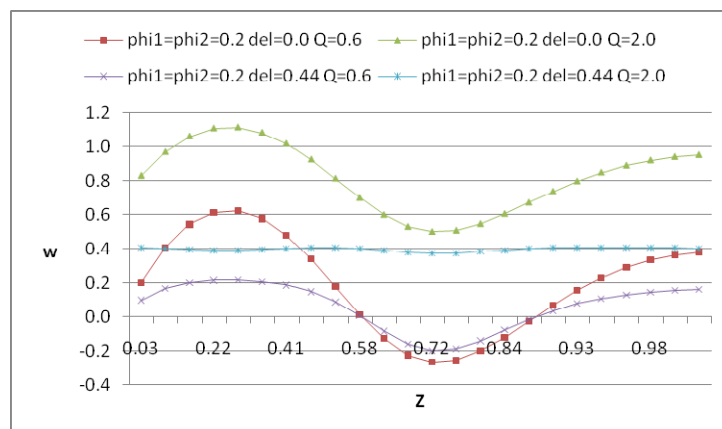


Figure 18. The same as in Figure 16, but for w versus Z at $r=0.5$.

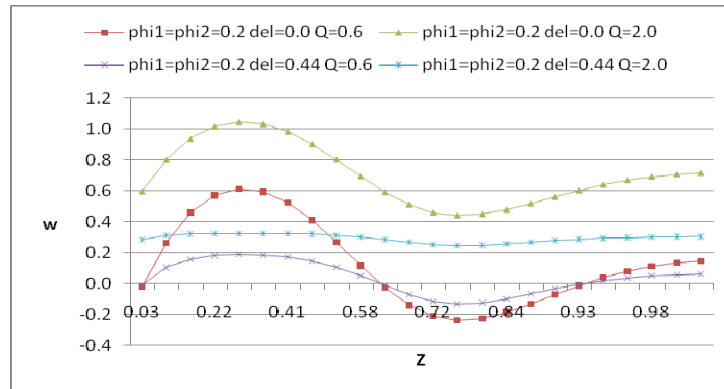


Figure 19. The same as in Figure 17, but for w versus Z at $r = 0.5$.